

## Section IV

# Quasar and Supermassive Black Hole Demographics

*Chair: Rachel Somerville*

# Black Hole Demographics: Statistical Characteristics of Accreting Black Holes

Hagai Netzer<sup>1</sup>

<sup>1</sup>School of Physics and Astronomy, Tel Aviv University, Tel Aviv 69978, Israel  
Email: netzer@wise.tau.ac.il

**Abstract.** This review summarizes the important properties of active black holes (BHs) up to  $z \sim 2$ ; their mass, accretion rate, and growth rate. At higher redshifts, such information is only available for small samples that do not represent the entire population of active galactic nuclei (AGNs). Black hole spin is still unknown; it is speculated to change with redshift, but with little experimental evidence. The available data sets also enable a direct comparison of BH accretion rates and host galaxy star-formation rates (SFRs). The ratio of the BH growth rate  $g(\text{BH})$  and the bulge growth rate  $g(\text{bulge})$ , suggests that the two are proportional to each other. The local value of  $g(\text{bulge})/g(\text{BH})$  in low-luminosity AGNs is of order 100 and the corresponding ratio in high-luminosity, high-redshift AGNs is of order 10. This has important implications regarding the parallel evolution of active BHs and their hosts.

**Keywords.** galaxies: active, galaxies: evolution, galaxies: nuclei

---

## 1. Introduction: Back to the Popper Way

This review addresses the statistical characteristics of black holes (BHs) in active galactic nuclei (AGNs). I shall comment on the merits and the difficulties of several mass determination methods but will not discuss, in a direct way, the  $M_{\text{BH}}-\sigma_*$  relationship or the reverberation mapping (RM) method, which are covered by Peterson (these proceedings) and others.

A major aim of this meeting is to uncover the time-dependent evolution of active BHs, from the onset of accretion in the first BHs to accreting BHs at  $z = 0$ . In principle, accurate BH mass functions, BH luminosity functions, and BH spin distributions at all redshifts can be used to infer the entire evolution of AGNs. We can start from the present epoch, with the known luminosity, mass and spin distributions, and proceed to larger and larger redshifts, incrementing, at each step, all three functions such that they agree with their properties at earlier times. Obviously, this kind of information is not yet available at all redshifts. Moreover, at high redshifts we usually know only the *mean population properties*, which are not sufficient to trace the evolution of individual BHs. Having a complete description of the accreting BH population at all redshifts will enable us to tie these properties with similar information of the entire galaxy population. Here I shall address only the connection of AGNs with star-forming (SF) galaxies.

This review does not follow the usual style of introducing the data and known correlations and posing a list of outstanding questions. Instead, I shall follow Karl Popper's approach, introducing in each section a declaration or a statement to see if it can be falsified. This, in my opinion, is the "correct" way of doing science.

## 2. Black Hole Mass

Popper's statement: *The mass distribution of active BHs is known at all redshifts (or: continuum luminosity and emission-line widths can be used to estimate, reliably, masses of active BHs at all redshifts).*

The masses of active BHs can be obtained in two ways. In type 1 AGNs, the broad-line region (BLR) size can be estimated from RM results that give the dependence of this size on the source luminosity. This is followed by assuming virialized cloud motion and using the width of certain broad emission lines to estimate cloud velocities (reviewed by Peterson in these proceedings). For type 2 AGNs, the stellar velocity dispersion in the host galaxy can be obtained from spectroscopic observations. This, plus the use of the "standard" (in fact, not so standard, see several contributions in this volume)  $M_{\text{BH}}-\sigma_*$  relationship provides the necessary estimate of  $M_{\text{BH}}$ . The use of this method is limited to low-redshift sources. The related  $M_{\text{BH}}-L(\text{galaxy})$  relationship can also be used. The above relationship cannot be used for disks or pseudo-bulges that are frequently found among AGN hosts.

### 2.1. The $H\beta$ Method

This is perhaps the best method for measuring  $M_{\text{BH}}$  in type 1 AGNs. It is based on the measurement of  $L_{5100}$  ( $\lambda L_\lambda$  at  $5100\text{\AA}$ ) and  $\text{FWHM}(H\beta)$ . Its advantage over other methods is the fact that most RM measurements are based on this continuum band and this emission line. The application of the method gives results that are in good agreement with the  $M_{\text{BH}}-\sigma_*$  method in AGN hosts where the stellar velocity dispersion has been measured.

### 2.2. The $Mg\text{II}\lambda 2798$ Method

This method is based on the combination of  $\text{FWHM}(Mg\text{II})$  and the luminosity of the  $3000\text{\AA}$  continuum. The results are almost as accurate as those based on the  $H\beta$  method. This can be verified by comparing the results in sources where both lines and both continuum bands are observed. Such a comparison has been performed in a large number of Sloan Digital Sky Survey (SDSS) sources (e.g., Shen *et al.* 2008).

### 2.3. The $C\text{IV}\lambda 1549$ Method

The third method, which is required for all  $z > 2$  AGNs observed in the SDSS 3500–9000  $\text{\AA}$  band, is based on the  $1450\text{\AA}$  continuum and  $\text{FWHM}(C\text{IV})$ . The method is known to produce problematic results, probably due to a non-virial component in the profile of the  $C\text{IV}\lambda 1549$  emission line. This has been demonstrated in various papers (e.g., Baskin & Laor 2005). A direct comparison with  $M_{\text{BH}}$  estimates obtained with the  $Mg\text{II}$  method is given by Risaliti *et al.* (2009) who used the Shen *et al.* (2008) sample. These authors report scatter greater than a factor of ten in  $M(C\text{IV})$  for a given  $M(Mg\text{II})$ . Netzer *et al.* (2007a) made a detailed comparison of  $M(C\text{IV})$  and  $M(H\beta)$  by fitting the  $C\text{IV}$  profile in several SDSS sources and comparing with  $M(H\beta)$  obtained from NIR spectroscopy of the same sources. Here, again, the range of  $M(C\text{IV})$  for a given  $M(H\beta)$  is about a factor of ten with no indication of a clear correlation of the two. Somewhat different results with better agreement between the methods are given by Vestergaard & Peterson (2006).

### 2.4. RM Revisited: The Role of Radiation Pressure Force

A recent work by Marconi *et al.* (2008) introduced an additional complication, and a source of a large potential uncertainty, into the RM mass estimate method. These authors considered the role of radiation pressure force in accelerating the BLR clouds. The importance of radiation pressure has been noted in numerous earlier BLR papers starting

with the seminal work of Mathews (1974). However, all earlier papers considered only ionized BLR and NLR gas and neglected gas clouds that are almost completely neutral. As argued by Marconi *et al.* (2008), in some of those cases, the “effective gravity” in some sources is considerably reduced compared to the case of pure virial motion, by the efficient radiation pressure force. This can change the derived value of  $M_{\text{BH}}$ .

The importance of radiation pressure acceleration can be computed accurately given a known ionization structure of the gas. It is most efficient when the entire medium is ionized since absorption by resonance lines can be very efficient. Bound-free absorption is the dominant factor in those cases where the resonance lines are optically thick. The net momentum delivered to the gas in such cases depends on the level of ionization and the continuum SED. The importance of radiation pressure acceleration, relative to gravity, depends on the column density of the gas. Gravity wins in large column density gas, where the continuum energy is absorbed only by the thin illuminated layer of ionized gas. Radiation pressure force is more important in lower column density gas. As noted by Marconi *et al.* (2008), in those AGNs with relatively low column density clouds, and with luminosities approaching the Eddington luminosity, radiation pressure can become the dominant force. This changes the shape of the line profiles significantly and results in smaller FWHM(H $\beta$ ) and hence underestimation of  $M_{\text{BH}}$ .

Consider the equation of motion

$$a(r) = a_{\text{rad}}(r) - g(r) - \frac{1}{\rho} \frac{dP}{dr} + \frac{f_{\text{d}}}{M_{\text{c}}} , \tag{2.1}$$

where  $a_{\text{rad}}$  is the acceleration due to radiation pressure,  $g$  is the gravitational acceleration,  $f_{\text{d}}$  is the drag force,  $M_{\text{c}}$  is the mass of a cloud and  $P$  is the gas pressure. Neglecting drag forces and thermal expansion, and assuming completely opaque gas, we can write the following expression for the acceleration of a “block,”

$$a(r) = \frac{L_{\text{bol}}}{r^2} \left[ \frac{a}{4\pi c m_{\text{p}} N_{\text{col}}} - \frac{G}{7.5 \times 10^4 (L_{\text{bol}}/L_{\text{Edd}})} \right] \tag{2.2}$$

where  $L_{\text{bol}}$  is the bolometric luminosity, the constant  $a$  contains information about the continuum SED and  $N_{\text{col}}$  is the cloud column density. The expression shows that the effective gravity is smaller than  $g(r)$  by an amount that depends mostly on the column density of the “block” (cloud). Solving for  $M_{\text{BH}}$  (which appears in the second term) we get

$$M_{\text{BH}} = a_1 V^2 L_{\text{bol}}^\alpha + a_2 \frac{L_{\text{bol}}}{N_{\text{col}}} . \tag{2.3}$$

The first term in this expression is the one used in the standard virial (“single epoch”) mass determination method. Here  $\alpha$  is of order 0.5 and  $V = f \times \text{FWHM}$  where  $f$  is of order unity (see Peterson, these proceedings). The second term is due to radiation pressure force.

Marconi *et al.* (2008) used the expression in equation (2.3) to solve for the constant  $a_1$  and the column density  $N_{\text{col}}$  that minimize the relationship between the RM-based mass determination and the virial (H $\beta$ -based) mass estimates in the original sample of Kaspi *et al.* (2000). Their best value for  $N_{\text{col}}$  was found to be almost exactly  $10^{23} \text{ cm}^{-2}$ . Given those values, they showed that the derived  $M_{\text{BH}}$  are much larger than those obtained with the simple virial method in sources of large  $L/L_{\text{Edd}}$ . Putting it differently, assuming  $N_{\text{col}} \sim 10^{23} \text{ cm}^{-2}$  for all AGNs, there are very few, if any, active BHs with  $L/L_{\text{Edd}} > 0.2$ .

While radiation pressure force must be important in at least some cases, three important issues must be raised:

- A reduced scatter is not, by itself, a sign of a better method of evaluating  $M_{\text{BH}}$ . The

introduction of an additional term that includes  $L_{\text{bol}}$  must result in a reduced scatter regardless of any additional assumption.

- Any realistic model of cloud motion must include the radial dependence of some of the cloud properties. For example, Rees, Netzer, & Ferland (1989) and later Netzer (1990) and Kaspi & Netzer (1999), show that under plausible assumptions about cloud confinement, the column density of a single cloud that retains its mass as it moves through the BLR is given by

$$N_{\text{col}} \propto r^{-2s/3}, \quad (2.4)$$

where  $s$  is a radial dependence parameter in the range 1–2. The column densities of such clouds are changing when moving in or out, which invalidates the concept of a simple “effective gravity.” Moreover, the factor  $a_2$  in equation (2.3) is, in itself, distance dependent, especially for small column density clouds. All this must be considered when calculating cloud motion and BH mass.

- There are several observational methods to test the Marconi *et al.* (2008) idea. The first is a direct comparison of BH properties in type 1 and type 2 samples.  $M_{\text{BH}}$  determination in type 2 AGNs is based on the  $M_{\text{BH}}-\sigma_*$  method and hence is independent of the BH gravity and the radiation pressure force. This can be used to compare BH mass and  $L/L_{\text{Edd}}$  distributions in type 1 and type 2 samples of similar properties. Such a comparison is discussed by Netzer (2009a) where it is argued that radiation pressure force is not very important in low- $z$  low luminosity AGNs (see also a refinement of the method by Marconi *et al.* 2009). Moreover, direct measurements of BLR cloud column densities are becoming available (Risaliti, these proceedings). Based on these studies, a typical column density in the BLR is a few times  $10^{23} \text{ cm}^{-2}$  or larger, which makes the effect of radiation pressure negligible.

To summarize, reliable BH mass estimates and hence BH mass functions are becoming available at all redshifts smaller than  $z \sim 2$ , where the  $\text{H}\beta$  and the  $\text{Mg II}$  methods can be used (see Vestergaard, these proceedings). This is not the case for large  $z > 2$  samples, where the highly uncertain C IV method has been used. Several small samples studied at NIR wavelengths produce reliable  $M_{\text{BH}}$  information, based on the  $\text{H}\beta$  and the  $\text{Mg II}$  methods, for a number of high-redshift, high-luminosity AGNs.

### 3. Accretion and Growth Rates

Popper’s statements: 1. *BH growth rates are known at all redshifts.* 2. *The first significant growth episode of the largest BHs occurred at  $z \sim 2-3$ .*

#### 3.1. Bolometric Correction

The observed AGN luminosity can be transformed directly to BH growth rate, given an efficiency (radiation conversion) factor  $\eta$  (note that I do not consider the “radio mode” where much of the accretion energy in the vicinity of the BH is released in the form of mechanical energy). Since much of the radiated energy is emitted in the unobserved FUV part of the spectrum, bolometric correction (BC) factors are required to properly estimate  $L_{\text{bol}}$ .

Various BC factors are commonly used. In type 1 AGN, they are usually based on the observed continuum luminosity. For low-redshift type 1 sources it is common to use  $L_{5100}$ . This gives a BC factor which ranges from about 11 for low-luminosity sources to about 6 in the most luminous AGNs. The equivalent BCs for the 3000 Å and the 1450 Å continua are about a factor of 1.5 and 2 smaller, respectively. The 2–10 keV continuum, thought

to be a clear AGN signature, can also be used by taking into account the well-known decrease in relative X-ray luminosity in higher-luminosity sources.

In type 2 sources, various emission-line luminosities, as well as the 2–10 keV luminosity, can be used with their appropriate BC factors. A line which is commonly used is [O III]  $\lambda$ 5007. This is usually among the strongest lines in the spectrum and is not contaminated by strong stellar absorption features. A direct comparison between Seyfert 1 and Seyfert 2 galaxies shows that for such sources,  $L_{\text{bol}}$  is some 3000 times larger than the observed  $L([\text{O III}] \lambda 5007)$  (e.g., Heckman *et al.* 2004; Netzer *et al.* 2006). For unattenuated, reddening-corrected line fluxes the conversion is roughly 400–1000, depending on the assumed extinction law.

Low-ionization type 2 AGN (type 2 LINERs; L2s) are very different in this respect. In such objects, the [O III]  $\lambda$ 5007 line reprocesses a considerably smaller fraction of the total luminosity because  $\text{O}^{+2}$  is not an abundant ion in the emitting gas. The conversion factor in such cases is close to 4000 (Netzer 2009b), a factor of 5–10 larger than in S1s. In such objects, the [O I]  $\lambda$ 6300 line is strong and a possible prescription based on the two oxygen lines that can be applied to both L2s and S2s is

$$\log L_{\text{bol}} = a_{\text{red}} + 0.75 \log L([\text{O I}] \lambda 6300) + 0.25 \log L([\text{O III}] \lambda 5007) , \quad (3.1)$$

where line luminosities are corrected for reddening and  $a_{\text{red}}$  is a factor which depends on the the extinction law. For galactic extinction,  $a_{\text{red}} \sim 3.8$  (Netzer 2009b).

### 3.2. $L/L_{\text{Edd}}$ distributions for Type 1 and Type 2 AGN

Having obtained estimates for  $M_{\text{BH}}$  and  $L_{\text{bol}}$ , we are now in a position to calculate  $L/L_{\text{Edd}}$  distributions for various subgroups of the AGN population. This has been done for several low and high redshift type 1 AGNs (e.g. Kollmeier *et al.* 2006; Netzer & Trakhtenbrot 2007; Netzer *et al.* 2007a; Shen *et al.* 2008; Gavignaud *et al.* 2008), but much less so for type 2 sources, mostly because of the difficulty in estimating  $L_{\text{bol}}$  and  $M_{\text{BH}}$  in high-redshift samples. The new  $L_{\text{bol}}$  estimate of equation (3.1) allows one to calculate  $L/L_{\text{Edd}}$  distributions for S2s, L2s in the data release four (DR4) type 2 Sloan digital sky survey (SDSS) sample. The sample contains thousands of spectra with a large range of signal-to-noise ratios ( $S/N$ ) and the examples shown here include only sources with  $S/N > 3$  in all emission lines under discussion. The resulting distributions are shown in Figure 1. As expected, the L2 and S2 distributions are very different, confirming the larger  $L/L_{\text{Edd}}$  in S2s (for a very detailed study of the ratio in many nearby sources with better  $S/N$ , see Ho 2009).

The differences between the L2 and S2 distributions is important for several reasons. First, most type 2 AGNs are LINERs and their proper treatment is essential in order to prevent biases in the estimate of the total (population) BH growth. This is not a trivial issue since LINERs are much fainter than high ionization Seyfert galaxies and flux-limited samples are likely to be more incomplete when counting such objects. Second, most if not all type 1 AGN samples observed with large entrance apertures (such as the SDSS with its 3-arcsec fiber) completely miss LINERs because of the difficulty in detecting their extremely faint broad emission lines against the stellar background. For example, Netzer (2009a) shows that the distribution of  $L/L_{\text{Edd}}$  in  $0.1 \leq z \leq 0.2$  S1s and S2s in the SDSS sample is very similar, but including L2s from the type 2 sample shifts the distribution to much smaller values of  $L/L_{\text{Edd}}$ .

A word of caution regarding BH mass estimates in type 2 AGNs is in place. The method used to obtain  $M_{\text{BH}}$  is based on the measured stellar velocity dispersion  $\sigma_*$  in the central  $3''$  of the host galaxy. This combined with the standard  $M_{\text{BH}}-\sigma_*$  relationship results in an  $M_{\text{BH}}$  estimate. However, this relationship does not apply to disk systems and

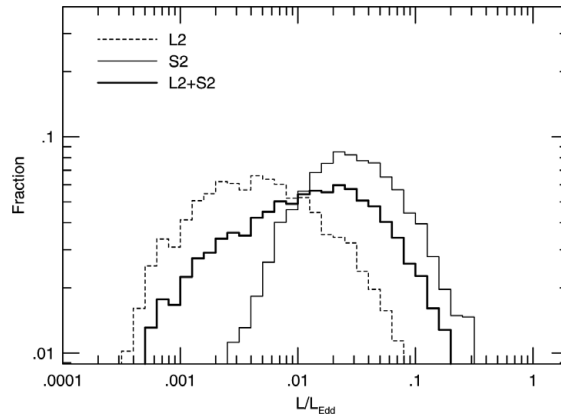


**Figure 1.**  $L/L_{\text{Edd}}$  distributions for S2s, L2s and the combined type 2 high  $S/N$  SDSS-DR4 sample.

to galaxies with pseudo-bulges. These are usually blue galaxies with enhanced SFR and their inclusion may bias the  $L/L_{\text{Edd}}$  distribution. A possible way to avoid this difficulty is to omit such galaxies from the sample by using color criteria like the SDSS  $u - r$  color. For example, following the procedure outlined by Baldry *et al.* (2004) which is based on  $u - r$ , I find that about 25% of the DR4 SDSS type 2 hosts belong to this group.

### 3.3. Black Hole Growth

Estimating BH growth rates is essential for studying the accumulation of mass in the centers of galaxies and for comparing BH and galaxy evolution. There are several possibilities regarding the growth mode. The one most commonly used assumes that once accretion starts, it continues at a constant relative rate,  $dM_{\text{BH}}/dt = \lambda M_{\text{BH}}$ . This leads to an equation of the form

$$t_{\text{grow}} = t_s \frac{\eta/(1-\eta)}{L/L_{\text{Edd}}} \ln \frac{M_{\text{BH}}}{M_{\text{seed}}}, \quad (3.2)$$

where  $t_s \approx 4 \times 10^8$  yrs. A possible justification for this assumption is that accretion proceeds at a rate which is close to the maximum allowed rate ( $L/L_{\text{Edd}} = 1$ ). In this case, the external mass supply exceeds the amount of mass that can be accreted by the BH.

A different possibility is a constant growth rate,  $dM_{\text{BH}}/dt = \text{constant}$ . This is perhaps more appropriate for a short growth phase with a constant external mass supply. A very interesting alternative is a growth rate that is proportional to the star-formation rate (SFR) in the host galaxy,  $dM_{\text{BH}}/dt = \beta \times \text{SFR}$ . In this case,  $t_{\text{grow}}$  depends on galaxy evolution in a way that can be estimated from numerical simulations.

The measured  $L/L_{\text{Edd}}$  enables a direct comparison of predicted and observed distributions of  $t_{\text{grow}}$ . Such a comparison is shown in Figure 2 where I plot  $t_{\text{grow}}/t_{\text{universe}}$  at two redshifts,  $z = 2.3$  and  $z = 3.4$ . In this case, the measured values of  $L/L_{\text{Edd}}$  are based on the  $H\beta$  method (NIR observations) and the assumed  $t_{\text{grow}}$  is given by equation (3.2). The diagram shows that even at such high redshifts, a large fraction of the sources show  $t_{\text{grow}}$  that is longer than the age of the universe at the appropriate redshift. Obviously, we are not witnessing the main accretion event, i.e., the one resulting in the accumulation of

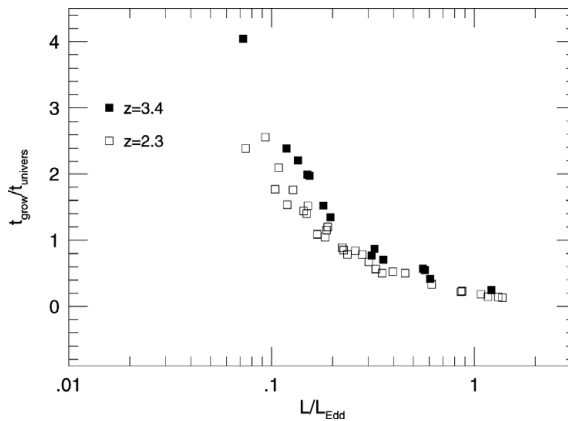


**Figure 2.** BH growth time relative to the age of the universe for  $z = 2.3$  and  $z = 3.4$  AGNs (Netzer *et al.* 2007a). About half of the sources did not have enough time to grow to their observed mass given their  $L/L_{\text{Edd}}$ .

most of the mass of the slowest growing BHs. Apparently, much of the growth of many BHs must have occurred at  $z > 3.4$  (see Trakhtenbrot *et al.*, these proceedings).

#### 4. Black Hole Spin

Popper's statement: *On average, BH spin is decreasing in time from close to the maximum allowed spin at high redshift to basically no rotation in the local universe.*

BH spin is extremely difficult to measure. In fact, except for a couple of low-redshift AGNs with extremely broad  $K\alpha$  lines (and even this has been disputed), there is no direct way to measure BH spin. Needless to say, the population properties are not known even at low redshift.

Perhaps the only way to assess the average BH spin at a given redshift is to study the evolution of  $\eta$ , the mass-to-luminosity conversion factor, with redshift. Basic BH theory suggests that the value of  $\eta$  can range from very large (about 0.4) for maximally rotating BHs to small (0.04) for retrograde rotation. As explained, the BH mass distribution (BH mass function) and luminosity distribution (AGN luminosity function), can be extrapolated in time from their known values at  $z = 0$  to larger and larger redshifts. The requirement for consistency with mass and luminosity functions at larger and larger redshifts involves an assumption about the mean value of  $\eta$ , and therefore the mean BH spin, at each redshift. Such studies are reported in several papers by Wang and collaborators (e.g., Wang *et al.* 2009) and by Rafiee and Hall (2009).

The recent Wang *et al.* (2009) work suggests a very large mean value,  $\langle \eta \rangle \sim 0.3$ , at  $z = 3$  and a much smaller value,  $\langle \eta \rangle \sim 0.04$ , at  $z = 0$ . This is hard to reconcile with basic ideas about expected changes in the direction of the angular momentum vector during separate accretion episodes. Unfortunately, the uncertainty in this method is very large, due mostly to the large uncertainties in the current BH mass and luminosity functions, especially at high redshift. This is an area where more progress is highly desirable because of the strong connection between  $\eta$  and the black hole growth time (equation 3.2).

#### 5. Accreting Black Holes and Star-Forming Hosts

Popper's statement: *BH growth rate is proportional to SFR at all redshifts.*



### 5.1. SFR in Type 1 AGNs

The best way to estimate SFR in type 1 AGN is by using the far infrared luminosity (FIR) of such sources. Several recent studies (Schweitzer *et al.* 2006; Netzer *et al.* 2007b; Lutz *et al.* 2008) indicate that most of the observed  $L(\text{FIR})$  in those sources is due to SF activity. Simple prescriptions allow the conversion of the observed IR luminosity to SFR with some uncertainty due to the lack of optical and UV information. Netzer *et al.* (2007b) and Lutz *et al.* (2008) show a clear and strong correlation between  $L(\text{FIR})$  and  $L_{\text{bol}}$  in high luminosity AGNs. Part of the correlation is due to a natural bias since some of the most luminous AGNs were chosen because they were known to show large submillimeter (SM) luminosity. However, other samples, especially the QUEST sample (part of the PG sample; see Schweitzer *et al.* 2006) were chosen by their optical color and the observed correlation cannot depend on their IR luminosity. Thus, there seems to be a strong correlation between  $L_{\text{bol}}$  and  $L_{\text{SF}}$  in type 1 AGNs.

### 5.2. SFR in Type 2 AGNs

Host galaxy properties, including SFR, are easier to measure and interpret in type 2 AGNs, since the strong optical–UV AGN continuum is obscured. Various methods to infer the SFR have been developed and several of those have been applied to SDSS type 2 samples (Kauffmann *et al.* 2003; Brinchmann *et al.* 2004; Heckman *et al.* 2004; Kewley *et al.* 2006; Groves *et al.* 2006; Salim *et al.* 2007; Wild *et al.* 2007; Kauffmann and Heckman 2009). They include an estimate based on  $L(\text{H}\alpha)$  (for SF dominated systems), the continuum break ( $D_{\text{n}}4000$ ) method, the UV–optical (*GALEX* observations) method, and the SED fitting method.

In general, there is good agreement between the  $D_{\text{n}}4000$  and the UV-color methods in objects with intense SFR but much poorer agreement for low SFR, typically older systems (Salim *et al.* 2007). For example, the two methods agree very well in young, small  $D_{\text{n}}4000$  systems but deviate, perhaps systematically, in hosts with  $D_{\text{n}}4000 > 1.8$  and/or very large stellar mass. The methods are also sensitive to the recipe used to correct the observed line intensity for dust attenuation (e.g., Wild *et al.* 2007). Nevertheless, it is possible to use the existing SDSS archive to estimate SFRs in thousands of type 2 hosts. This gives quite reliable SFR estimate for S2 hosts, where the SFR is high, and less reliable estimates for many L2 hosts that are more massive and characterized by an older stellar population.

### 5.3. Simple Evolutionary Schemes

Bolometric luminosity estimates and SFR estimates can be compared to test the assumption that the two are proportional to each other over a large luminosity range. This can be done by combining the estimates based on  $L(\text{FIR})$  in luminous type 1 AGNs with those of low-luminosity, type 2 sources that are based on the  $D_{\text{n}}4000$  and the UV–color methods. Such a comparison, covering almost five orders of magnitude in  $L_{\text{bol}}$ , is shown in Figure 3. Here the high-luminosity sources are taken from Netzer *et al.* (2007b) and Lutz *et al.* (2008) and the low-luminosity sources are from Netzer (2009b). The latter are grouped into bins of 0.1 dex in  $L_{\text{bol}}$ .

Figure 3 illustrates the clear correlation of  $L_{\text{bol}}$  and  $L_{\text{SF}}$  over almost five orders of magnitude in  $L_{\text{bol}}$ . While a standard correlation analysis cannot be performed because of the uneven distribution of sources with  $L_{\text{bol}}$  and the numerous upper limits, a correlation of the form  $L_{\text{SFR}} \propto L_{\text{bol}}^{\gamma}$ , with  $\gamma \sim 0.7\text{--}0.8$ , fits the data well. At the low-luminosity ( $\sim 10^{42}$  ergs  $\text{s}^{-1}$ ) end,  $L_{\text{SFR}} \sim L_{\text{bol}}$ . At the high-luminosity ( $10^{47}$  ergs  $\text{s}^{-1}$ ) end,  $L_{\text{SFR}} \sim 0.06L_{\text{bol}}$ . Note that the diagram shows the relationship of  $L_{\text{SF}}$  and  $L_{\text{bol}}$  in *AGN-dominated systems* i.e., those sources where most of the bolometric luminosity is due to BH accretion.

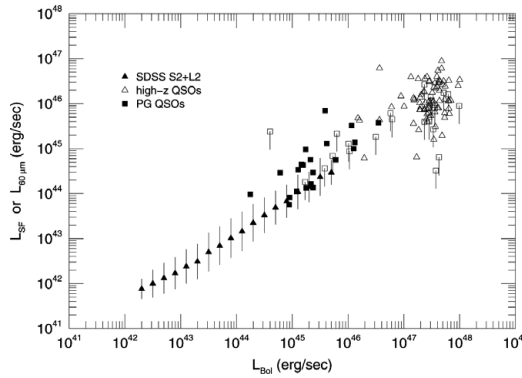


**Figure 3.**  $L_{SF}$  vs.  $L_{bol}$  for luminous type 1 and low luminosity type 2 AGNs (after Netzer 2009b). The type 2 objects are grouped in bins of 0.1 dex in  $L_{bol}$ .

Two regions in Figure 3 are almost empty and require further explanation. The top left part of the diagram contains no sources since only AGN-dominated objects were considered. Systems with a weak AGN and high SFR will occupy this area. In a simple scheme where the SF activity precedes the onset of the BH accretion rate by several Myr, this will be the location of sources whose BH accretion is still rising (note that pure SF galaxies will not appear at all on the diagram). The bottom right part of the diagram could, in principle, be the location of numerous sources with strong AGN activity yet small SFR. There are very few known sources with such properties (e.g., well-known but not so common luminous AGNs in large elliptical galaxies) and more of those can perhaps be found among the sources that currently have only upper limits on  $L_{SF}$ . Such sources are expected in flux-limited samples, yet their absence is not fully compatible with present IR capabilities. Future observations with *Herschel* can perhaps help locate more such sources.

In the following, I am going to assume that the differences between total stellar mass and bulge mass are not very large and the latter represents much of the stellar mass in the local universe. Since  $L_{SF}$  can be transformed into bulge growth rate, and  $L_{bol}$  can be transformed into BH growth rate, the two can be combined to give

$$\frac{g(\text{bulge})}{g(\text{BH})} \approx 110 \left[ \frac{\eta_{BH}/0.1}{\eta_{SF}/7 \times 10^{-4}} \right] \left[ \frac{L_{bol}}{10^{42} \text{ erg s}^{-1}} \right]^{-0.2}. \tag{5.1}$$

This means that at the bottom left part of the diagram, where  $L_{bol} \sim 10^{42} \text{ ergs s}^{-1}$ , the bulge growth rate exceeds the BH growth rate by a factor of about 110. The objects in this region are mostly low-luminosity local sources for which  $M(\text{bulge})/M_{BH} \sim 1000$  (more like 2000 for the total stellar mass in late-type galaxies). The difference between the two numbers (110 and 1000) can be reconciled by noting that most of the stellar growth rate in the local universe is occurring in SF galaxies that host no, or extremely weak, AGNs. For example, Salim *et al.* (2007) find that about 8/9 of the total bulge growth at redshift zero is due to such systems. This factor is in accord with equation (5.1), assuming we are witnessing the main growth episode of such sources.

The situation at the high-luminosity, high-redshift end is very different. At this end  $g(\text{bulge})/g(\text{BH})$  is of order 10–20, i.e., some 50 times slower than its cosmic average value. A naive explanation is that for those sources most of the BH growth has already occurred. For those sources, later stages of evolution will be characterized by longer SF episodes compared with the BH growth episodes (i.e., the BH and SF duty cycles are evolving in time).

**References**

- Baldry, I. K., Glazebrook, K., Brinkmann, J., Ivezić, Ž., Lupton, R. H., Nichol, R. C., & Szalay, A. S. 2004, *ApJ*, 600, 681
- Baskin, A. & Laor, A. 2005, *MNRAS*, 358, 1043
- Brinchmann, J., Charlot, S., White, S. D. M., Tremonti, C., Kauffmann, G., Heckman, T., & Brinkman, J. 2004, *MNRAS*, 351, 1151
- Gavignaud, I., *et al.* 2008, *A&A*, 492, 637
- Groves, B., Kewley, L., Kauffmann, G., & Heckman, T. 2006, *New Astronomy Reviews*, 50, 743
- Heckman, T. M., Kauffmann, G., Brinchmann, J., Charlot, S., Tremonti, C., & White, S. D. M. 2004, *ApJ*, 613, 109
- Ho, L. 2009, *ApJ*, 699, 626
- Kaspi, S. & Netzer, H. 1999, *ApJ*, 524, 71
- Kaspi, S., Smith, P. S., Netzer, H., Maoz, D., Jannuzi, B. T., & Giveon, U. 2000, *ApJ*, 533, 631
- Kauffmann, G., *et al.* 2003, *MNRAS*, 346, 1055
- Kauffmann, G. & Heckman, T. M. 2009, *MNRAS*, 397, 135
- Kewley, L., *et al.* 2006, *MNRAS*, 372, 961
- Kollmeier, J. A., *et al.* 2006, *ApJ*, 648, 128
- Lutz, D., Sturm, E., Tacconi, L. J., Valiante, E., Schweitzer, M., Netzer, H., Maiolino, R., Andreani, P., Shemmer, O., & Veilleux, S. 2008, *ApJ*, 684, 853
- Marconi, A., Axon, D. J., Maiolino, R., Nagao, T., Pastorini, G., Pietrini, P., Robinson, A., & Torricelli, G. 2008, *ApJ*, 678, 693,
- Marconi, A., Axon, D., Maiolino, R., Nagao, T., Pietrini, P., Robinson, A., & Torricelli, G. 2009, *ApJ*, 698, 103
- Mathews, W. G. 1974, *ApJ*, 189, 23
- Netzer, H. 1990, in *Active Galactic Nuclei*, Saas-Fee Advanced Course 20, ed. T. J.-L. Courvoisier & M. Mayor (Berlin: Springer)
- Netzer, H., Mainieri, V., Rosati, P., & Trakhtenbrot, B. 2006, *A&A*, 453, 525
- Netzer, H., & Trakhtenbrot, B. 2007, *ApJ*, 654, 754
- Netzer, H., Lira, P., Trakhtenbrot, B., Shemmer, O., & Cury, I. 2007a, *ApJ*, 671, 1256
- Netzer, H., *et al.* 2007b, *ApJ*, 666, 806
- Netzer, H. 2009a, *ApJ*, 695, 793
- Netzer, H. 2009b, *MNRAS*, 399, 1907
- Rafiee, A. & Hall, P. B. 2009, *ApJ*, 691, 425
- Rees, M. J., Netzer, H., & Ferland, G. J. 1989, *ApJ*, 347, 640
- Risaliti, G., Young, M., & Elvis, M. 2009, *ApJ*, 700, L6
- Salim, S., *et al.* 2007, *ApJS*, 173, 267 (S07)
- Shen, Y., Greene, J. E., Strauss, M. A., Richards, G. T., & Schneider, D. P. 2008, *ApJ*, 680, 169
- Schweitzer, M., *et al.* 2006, *ApJ*, 649, 79
- Vestergaard, M. & Peterson, B. M. 2006, *ApJ*, 641, 689
- Wang, J.-M., *et al.* 2009, *ApJ*, 697, L141
- Wild, V., Kauffmann, G., Heckman, T., Charlot, S., Lemson, G., Brinchmann, J., Reichard, T., & Pasquali, A. 2007, *MNRAS*, 381, 543